Journal of Sustainable Development of Energy, Water and Environment Systems

http://www.sdewes.org/jsdewes

Year 2026, Volume 14, Issue 4, 1140747

Original Research Article

Optimal Sizing and Power System Analysis of Hybrid Renewable Energy Systems for Sustainable Tourism in Mangrove Regions Using HOMER Pro and DIgSILENT PowerFactory

Md Abu Rayhan[1], Akhlaqur Rahman[2], Hadiuzzaman Hadiuzzaman[1], Sk. A. Shezan[*3], Md. Fatin Ishraque[4], Ezzeddine Touti[5]

[1]Department of Electrical and Electronic Engineering, Green University of Bangladesh, Dhaka, Bangladesh.
e-mail: aburayhan.contact@gmail.com; hadiuzzaman381@gmail.com

[2]Department of Electrical Engineering and Industrial Automation, Engineering Institute of Technology, Melbourne Campus, Australia.
e-mail: akhlaqur.rahman@eit.edu.au

[3]Department of Electrical Engineering, Prince Faisal bin Khalid bin Sultan Research Chair in Renewable Energy Studies and Applications (PFCRE), Northern Border University, Arar, KSA.
e-mail: shezan@nbu.edu.sa

[4]Department of Electrical, Electronic and Communication Engineering, Pabna University of Science and Technology, Pabna, Bangladesh.
e-mail: fatineeeruet@gmail.com

[5]Center for Scientific Research and Entrepreneurship, Northern Border University, Arar 73213, Saudi Arabia
e-mail: esseddine.touti@nbu.edu.sa

Corresponding Author: Sk. A. Shezan (shezan@nbu.edu.sa)

Cite as: Rayhan, M. A., Rahman, A., Hadiuzzaman, H., Shezan, S. A., Ishraque, M. F., Touti, E., Optimal Sizing and Power System Analysis of Hybrid Renewable Energy Systems for Sustainable Tourism in Mangrove Regions Using HOMER Pro and DIgSILENT PowerFactory, J.sustain. dev. energy water environ. syst., 14(4), 1140747, 2026, DOI: https://doi.org/10.13044/j.sdewes.d14.0747

ABSTRACT

Remote mangrove ecotourism sites, constrained by environmental sensitivity and limited grid access, rely on costly, polluting diesel generators. This study designs and validates hybrid renewable energy systems for sustainable tourism in the Sundarbans (Bangladesh), Can Gio (Vietnam), and Guaratiba (Brazil). Using HOMER Pro, system sizing and long-term costs are optimised on the basis of local solar, wind and biomass resources and multi-sector electricity demand, while DIgSILENT PowerFactory is used to verify steady-state and dynamic performance through load-flow and fault analyses. The optimised hybrid systems achieve 80–85% renewable penetration, with the Sundarbans leading due to strong wind and biomass resources, and reduce total energy costs by 22–35% and greenhouse gas emissions by more than 70% compared to diesel-only supply. Across the three sites, the levelized cost of energy falls in the range of approximately 0.11–0.21 USD/kWh, versus more than 0.30 USD/kWh for existing diesel-based generation, while the contribution of diesel generation is greatly reduced, consistent with the large decrease in associated emissions. Voltage deviations remain within ±5% of nominal levels, line loadings stay below thermal limits and fault recovery under 2 seconds, indicating that the proposed configurations can provide reliable and resilient power under disturbed operating conditions. Overall, the integrated HOMER–DIgSILENT framework offers a scalable model for planning low-carbon electrification of ecologically sensitive mangrove regions, supporting progress towards Sustainable Development Goals 7 (affordable and clean energy), 8 (decent work and economic growth), 9 (industry, innovation and infrastructure), 13 (climate action) and 15 (life on land), while enhancing local energy security and sustainability.

KEYWORDS

Hybrid Renewable Energy Systems, Mangrove Ecotourism, Techno-Economic Optimization, Reliability Analysis, Sustainable Electrification.

INTRODUCTION

Mangrove ecosystems are among the most carbon-rich and ecologically significant environments globally, providing essential services such as coastal protection, biodiversity conservation, and support for fisheries and local livelihoods [1], [2]. In recent years, these regions have also emerged as important ecotourism destinations, contributing to sustainable economic development. However, their remote locations and environmentally sensitive characteristics pose significant challenges for the provision of reliable and sustainable energy infrastructure.

Electricity supply in such regions is typically dominated by diesel-based generation, which is associated with high operational costs, fuel transportation constraints, and considerable greenhouse gas emissions [3]. These limitations undermine the environmental sustainability of ecotourism and conflict with global development priorities such as access to clean energy and climate action. Moreover, electricity demand in mangrove ecotourism regions is inherently complex, involving multiple interacting sectors including residential users, tourism facilities, agriculture and aquaculture activities, and emerging electric mobility applications. This results in highly variable and temporally dynamic load profiles that are difficult to serve efficiently using conventional single-source generation systems.

Hybrid renewable energy systems (HRES), integrating resources such as solar, wind, biomass, and energy storage, have been widely investigated as a viable solution for remote and off-grid electrification. Numerous studies have demonstrated the economic and environmental advantages of such systems using techno-economic optimization tools, particularly HOMER Pro. For example, Uddin et al. [4] and Ali et al. [5] reported significant reductions in system cost and emissions through optimized hybrid configurations, while Shezan et al. [6] highlighted the application of hybrid systems in tourism-based energy supply. Similarly, Islam et al. [7] and Faisal and Anwer [8] demonstrated the feasibility of solar–wind hybrid systems in coastal and rural contexts, and Ahmed et al. [9] and Prasetyo et al. [10] extended such analyses to healthcare and public infrastructure applications. Additional studies, including AbdElrazek et al. [11] and Samatar et al. [12] further emphasized the potential of hybrid systems for emission reduction and sustainable energy supply across different sectors. Despite these advances, several critical limitations remain in the existing literature. Most studies focus primarily on techno-economic optimization and do not incorporate detailed electrical performance validation. In contrast, power system studies using tools such as DIgSILENT PowerFactory have addressed issues related to network stability, distributed generation integration, and fault behaviour [13], [14], but typically assume predefined system configurations without considering optimal system sizing. Furthermore, many studies rely on simplified or single-sector load representations, which do not adequately capture the multi-sector demand characteristics of ecotourism-driven coastal regions. In addition, analyses are often limited to single locations and use aggregated or low-resolution data, reducing their applicability to complex, real-world systems.

A concise overview of relevant hybrid-system applications is presented in **Table 1**, which summarises system configurations, main results and limitations for studies most relevant to fragile ecotourism or remote coastal regions. Several of these studies report levelized cost of energy (LCOE) in the range of approximately 0.14–0.24 USD/kWh for optimised hybrid microgrids serving remote or islanded communities, often with substantial diesel displacement and greenhouse gas reductions. For example, Islam et al. [15] demonstrated an LCOE of about 0.19 USD/kWh for a zero-emission PV–wind–battery system in a Canadian coastal community, while Jahangir and Cheraghi [16] reported an LCOE of roughly 0.17 USD/kWh and 68% CO_2 reduction for a solar–wind–biomass hybrid in a rural settlement. He et al. [17] analysed a remote island hybrid system that reduced diesel use by more than 60% with an LCOE around 0.20 USD/kWh, and El Hassani et al [18] confirmed stability in hybrid PV–wind–hydrogen systems in an islanded with fault recovery within 3 seconds. Tourism-oriented and coastal

studies, such as those by Shezan et al. [6] and Palanichamy et al. [19], further demonstrate diesel reductions of 40–45% through hybridisation, while Ayan & Turkay [20] and Barakat et al. [21] highlight how optimised PV–wind systems can achieve competitive LCOE ranges and improved reliability in diverse climatic conditions. Ali et al. [22] showed that storage often accounts for 30–40% of system costs, underscoring the importance of careful battery sizing. However, many of these systems rely on standardised, medium-scale technologies and relatively larger loads than those considered in the present work, which focuses on smaller, non-standard hybrid systems in environmentally sensitive mangrove regions.

Table 1. Comparative summary of relevant studies on hybrid renewable energy systems, highlighting application

Study	Application/Location	Configuration	Main Result	Limitation
Uddin et al. [4]	Coastal Bangladesh	PV–Wind–Diesel	20% cost reduction	No consideration of mangrove-specific constraints
Ali et al. [5]	University campus, Bangladesh	PV–Biomass	25% LCOE reduction	Grid stability not assessed
Shezan et al. [6]	Resort, Malaysia	PV–Wind–Biomass	Optimized hybrid configuration	Ignored dynamic tourism loads
Islam et al. [15]	Coastal, Canada	PV-Wind-Battery	LCOE 0.19 USD/kWh, zero-emission	Context-specific
Jahangir & Cheraghi [16]	Rural settlement	PV–Wind–Biomass	68% CO_2 reduction, LCOE ≈ 0.17 USD/kWh	No tourism load consideration
He et al [17]	Remote island	PV–Wind–Battery	60% diesel reduction, LCOE ≈ 0.20 USD/kWh	Storage limitations
El Hassani et al. [18]	Morocco (island)	PV–Wind–Hydrogen	Stable under 3-phase fault (<3s)	High H_2 storage cost
Palanichamy et al. [19]	Secluded settlement, India	PV–Wind–Diesel	45% diesel reduction	Small-scale application
Ayan & Turkay [20]	7 climate regions, Turkey	PV–Wind–Diesel	LCOE range 0.14–0.24 USD/kWh	Generic loads assumptions
Ali et al [22]	Review (storage)	Multiple	Storage 30–40% system cost	No site-specific validation
Barakat et al [21]	Urban microgrid	PV–Wind–Battery	15% LCOE reduction, improved reliability	Urban-focused context
Kumar et al. [23]	Tool review	HOMER, DIgSILENT	Tools complement each other	No case study
Ahmed et al. [24]	Suburban community microgrid, Bangladesh	HOMER Pro, DIgSILENT	Techno-economic sizing with validated outage stability	Not focused on coastal or tourism-based systems

Consequently, there remains a lack of integrated frameworks that simultaneously address multi-sector demand modelling, multi-resource hybrid system optimization, and detailed power system reliability assessment within a unified approach. This gap is particularly relevant for environmentally sensitive and tourism-dependent regions, where both economic performance and electrical reliability are critical for sustainable development. Based on this research gap, this study hypothesizes that the integration of multi-resource hybrid renewable energy systems with combined techno-economic optimization and power system reliability analysis can provide a cost-effective and technically feasible solution for electrifying multi-sector mangrove ecotourism regions, significantly reducing dependence on diesel-based generation while ensuring acceptable steady-state and dynamic network performance.

To test this hypothesis, a comprehensive methodological framework is developed that incorporates sector-based load modelling, renewable resource assessment, techno-economic optimization, and power system reliability analysis. Hybrid configurations including

photovoltaic, wind, biomass, and battery energy storage systems are evaluated using HOMER Pro, while their electrical feasibility is assessed through load-flow and fault analyses in DIgSILENT PowerFactory. This integrated approach enables simultaneous evaluation of economic efficiency and network operability, addressing key limitations of previous single-domain studies.

The remainder of the paper is structured as follows. The methodology section presents the overall framework, including load modelling, renewable resource assessment, techno-economic optimization, and reliability analysis. The results and discussion section presents the key findings, while the conclusions section summarizes the main outcomes, limitations, and future research directions.

METHODOLOGICAL APPROACH

This study develops a generalized methodological framework for the optimal design and technical validation of hybrid renewable energy systems (HRES) in remote and environmentally sensitive regions with multi-sector electricity demand. The framework integrates techno-economic optimization with power system reliability analysis to ensure that cost-optimal system configurations are also electrically feasible under realistic operating conditions.

Previous studies have typically addressed these aspects separately. Techno-economic optimization using tools such as HOMER Pro has been widely applied to identify least-cost system configurations [4], while power system simulation tools such as DIgSILENT PowerFactory have been used to evaluate network performance and stability [13, 14]. However, the lack of integration between these approaches limits the ability to ensure that economically optimal solutions satisfy electrical network constraints.

The proposed methodology addresses this gap by coupling optimization and validation in a sequential framework. First, candidate hybrid system configurations are optimized using techno-economic criteria. Second, the resulting configurations are evaluated through detailed electrical network modelling to verify steady-state feasibility and operational robustness. This approach ensures methodological consistency and improves the reliability of system design outcomes.

A schematic representation of the methodological workflow is provided in
Figure 1**.**

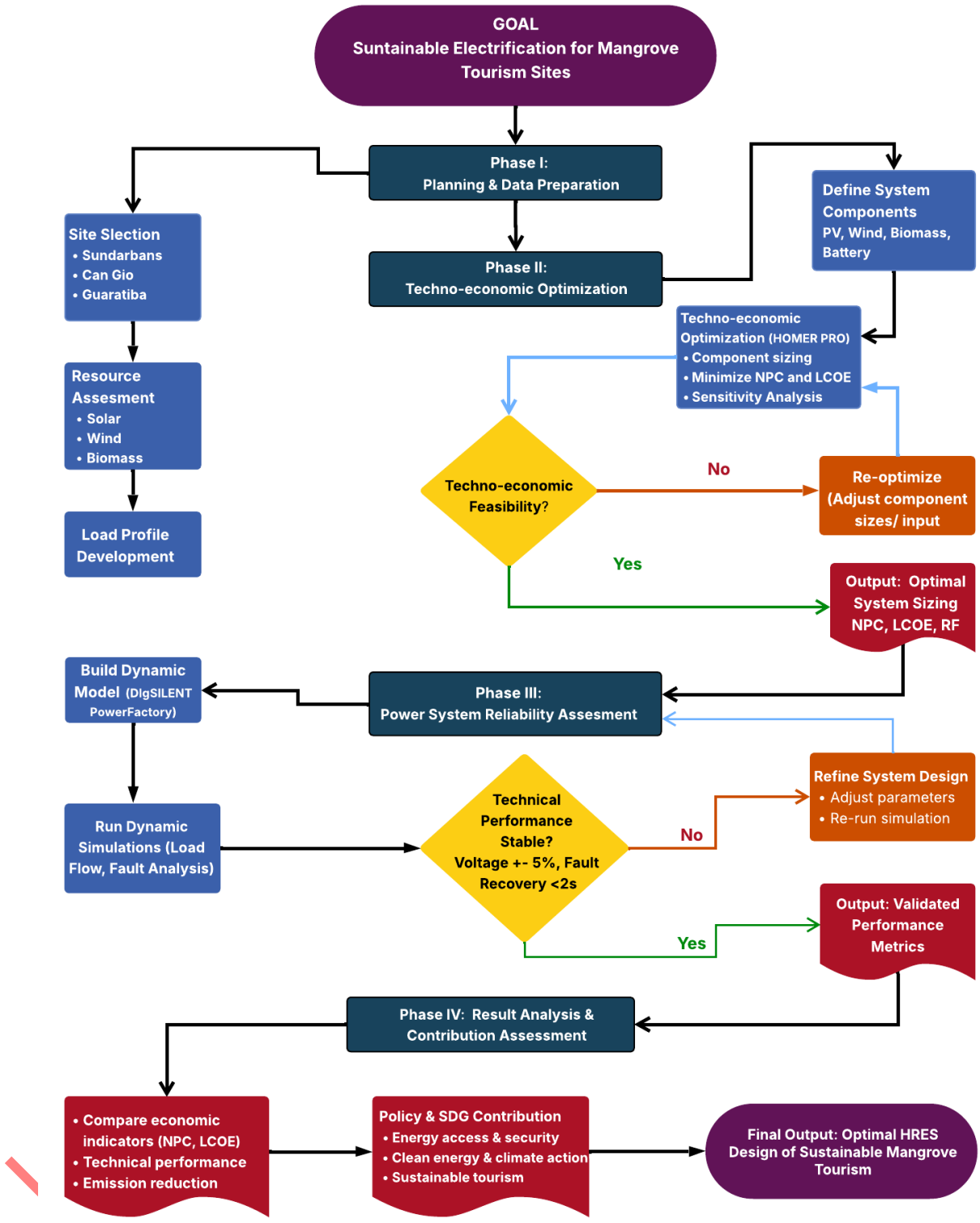

Figure 1. Methodological Flowchart for Optimal Design and Evaluation of Hybrid Renewable Energy Systems for Sustainable Mangrove Tourism.

Load Modelling

Electricity demand is modelled using a sector-based bottom-up approach, which is appropriate for coastal and ecotourism-oriented regions where detailed metered data are rarely available [25], [26]. The total demand is represented as the aggregation of residential and tourism accommodation loads, agricultural and aquaculture loads, small-scale industrial and service loads, and electric mobility demand.

Previous studies on isolated and weak-grid coastal communities report typical residential electricity consumption in the range of 1.5–2.5 kWh per household per day, depending on appliance ownership and service level. Tourism facilities generally exhibit higher consumption levels due to refrigeration, air-conditioning and service equipment, and are therefore treated as a distinct load category [25], [27]. Tourism facilities such as eco-lodges and guest houses exhibit higher energy consumption due to refrigeration, air-conditioning, and service equipment, and are therefore treated as a distinct sub-category within the residential sector [6], [19].

Agricultural and aquaculture electricity demand is characterized based on typical operating characteristics of small irrigation and pumping systems. Reported daily electricity requirements commonly fall within the range of 5–10 kWh per pump, depending on motor capacity and operating duration [27], [28]. Industrial and service loads, including fish processing units, ice plants, and cold storage facilities, are represented using reported daily energy demands of approximately 150–250 kWh per unit for small coastal facilities [29], [30]. Electric mobility demand is incorporated to reflect the increasing adoption of electric boats and shuttle vehicles in sustainable tourism contexts. Reported specific energy consumption values for light electric vehicles and short-range transport are used to define representative daily charging demand ranges [31].

Hourly load profiles are constructed by assigning normalized temporal demand shapes to each sector based on typical usage patterns reported in the literature [26], [27]. These normalized profiles are subsequently scaled using sectoral daily energy ranges and aggregated to obtain composite hourly load curves. This approach ensures methodological transparency and allows the load modelling procedure to be replicated for other regions with different site-specific inputs.

Renewable Resource Assessment

Renewable resource assessment is conducted for solar, wind, and biomass energy using long-term datasets obtained from publicly accessible sources, including global solar and wind atlases and national meteorological databases [32], [33]. These datasets provide representative monthly and annual averages suitable for regional-scale hybrid system planning.

Solar resource characterization is based on global horizontal irradiance (GHI) data, which are widely used in hybrid system studies [33], [34]. Long-term average GHI values are combined with representative diurnal and seasonal variation patterns to generate synthetic hourly solar irradiance time-series suitable for optimization in HOMER Pro.

Wind resource assessment relies on mean wind speed data at reference heights obtained from global wind atlases [32], [35]. Wind speeds are extrapolated to the assumed turbine hub height using standard vertical wind profile models appropriate for coastal terrain [32]. Hourly wind speed time-series are then converted to electrical power using representative turbine power curves, consistent with previous hybrid microgrid studies [36].

Biomass resource assessment follows a residue-based approach, in which locally available organic by-products from forestry, agriculture, and aquaculture activities are identified [28], [37]. Reported residue-to-product ratios and lower heating values are used to estimate the potential daily energy contribution from biomass resources [36], [38]. These estimates are treated as upper bounds on dispatchable biomass energy rather than fixed generation values. Detailed cost parameters and assumptions used in the HOMER Pro optimization are provided in **Appendix 1.**

Techno-economic Optimization

Techno-economic optimization of the hybrid renewable energy systems is performed using HOMER Pro, a widely applied commercial software for the planning of off-grid and microgrid systems [39], [40]. HOMER Pro simulates system operation at an hourly resolution over the

project lifetime and evaluates multiple technology combinations to identify cost-optimal solutions.

Similar optimization approaches using HOMER Pro have been reported for community microgrids, tourism facilities, and coastal hybrid systems, demonstrating its suitability for evaluating cost, emissions, and renewable penetration [4], [41]. Candidate system configurations include photovoltaic arrays, wind turbines, biomass-based generators, battery energy storage systems, power converters, and diesel generators for backup where applicable.

Objective Functions and Economic Performance Indicators. The optimization objective is to minimize the net present cost (NPC) of the system, which accounts for capital investment, replacement costs, operation and maintenance expenses, fuel costs, and salvage values over the project lifetime [39], as given in **Equation (1)**:

$$NPC = \sum_{t=1}^{N} \frac{C_t}{(1+r)^t} \quad (1)$$

The LCOE is calculated by dividing the NPC by the total discounted electrical energy supplied over the project lifetime [4], [5] as given in **Equation (2)**:

$$LCOE = \frac{NPC}{\sum_{t=1}^{N} \frac{E_t}{(1+r)^t}} \quad (2)$$

The renewable energy fraction (RF) is defined as the ratio of energy generated from renewable sources to the total energy served, a metric commonly used in hybrid system studies to quantify renewable penetration [6], [41], as given in **Equation (3)**:

$$RF = \frac{E_{PV} + E_{wind} + E_{biomass}}{E_{served}} \quad (3)$$

Sensitivity analyses are performed by varying key economic parameters, such as fuel price, discount rate, and battery replacement cost, to assess the robustness of the optimization results [5], [41]. The notation used in **Equations (1), (2), and (3)** are summarized in

Appendix 2**.**

Power System Reliability Analysis

The power system reliability of the optimised hybrid renewable energy systems was evaluated using DIgSILENT PowerFactory, which provides a detailed electrical network simulation environment for steady-state and dynamic analyses. The techno-economically optimal configurations obtained from HOMER Pro were implemented as equivalent generation and load models within the DIgSILENT framework to assess network feasibility and operating robustness.

The overall electrical network structure adopted for the reliability assessment, including generation units, storage systems, loads, transformers and interconnections, is illustrated in **Figure 2.**

Network Modelling and Steady-State Load Flow Analysis. Each case study system was modelled as a multi-voltage distribution network comprising buses, lines, transformers, generators, storage units and aggregated loads, following the schematic layout shown in **Figure 2.** The network represents a hierarchical voltage structure, with generation and storage units connected at low-voltage levels and interfaced to the national grid through appropriate step-up transformers. Generation units representing photovoltaic arrays, wind turbines and biogas generators were connected to suitable buses according to the adopted system topology.

Battery energy storage systems were modelled through converter-interfaced storage units, while an electric vehicle charging station (EVCS) was explicitly represented as a dedicated load node within the network, as shown in **Figure 2**. Loads were modelled as constant-power demands with fixed power factors, ensuring consistent active and reactive power requirements during steady-state operation.

Steady-state operating points were obtained using the Newton–Raphson load flow algorithm implemented in DIgSILENT PowerFactory. The load flow solution enforces active and reactive power balance at each bus while respecting network constraints such as voltage limits, line thermal ratings and generator operating bounds. Voltage magnitudes, line loading levels, and active and reactive power losses were extracted to verify that the optimized system configurations satisfy standard distribution network performance criteria.

For steady-state load flow analysis, dynamic models and transient controllers were deactivated, ensuring that the results reflect static operating conditions without the influence of dynamic control actions. Dynamic simulations related to fault events were conducted separately and are presented in the results section.

Control Strategy and Load Flow Solution Logic. DIgSILENT PowerFactory was employed to determine feasible steady-state operating conditions rather than to perform global techno-economic optimization. Control strategies were implemented through predefined generator and converter control modes, including fixed power-factor operation and active power dispatch consistent with the HOMER Pro optimization results. Battery units were modelled to inject or absorb power according to their scheduled operating points, without participating in dynamic frequency or voltage control during steady-state analysis.

The load flow solution iteratively adjusts bus voltages and power flows until convergence is achieved within specified numerical tolerances. Operating points that violate voltage, loading or power balance constraints are considered infeasible. This procedure ensures that the optimized hybrid configurations are not only cost-effective but also electrically operable under nominal conditions.

Rationale for the Adopted Modelling Approach. The combined use of HOMER Pro and DIgSILENT PowerFactory enables a clear separation between techno-economic optimization and electrical performance validation. HOMER Pro is used to identify cost-optimal system configurations based on long-term energy balances, while DIgSILENT PowerFactory verifies that these configurations can operate reliably within realistic network constraints, as represented by the network model in **Figure 2.** This sequential approach enhances methodological transparency and reproducibility by avoiding the conflation of optimization procedures with power system simulation.

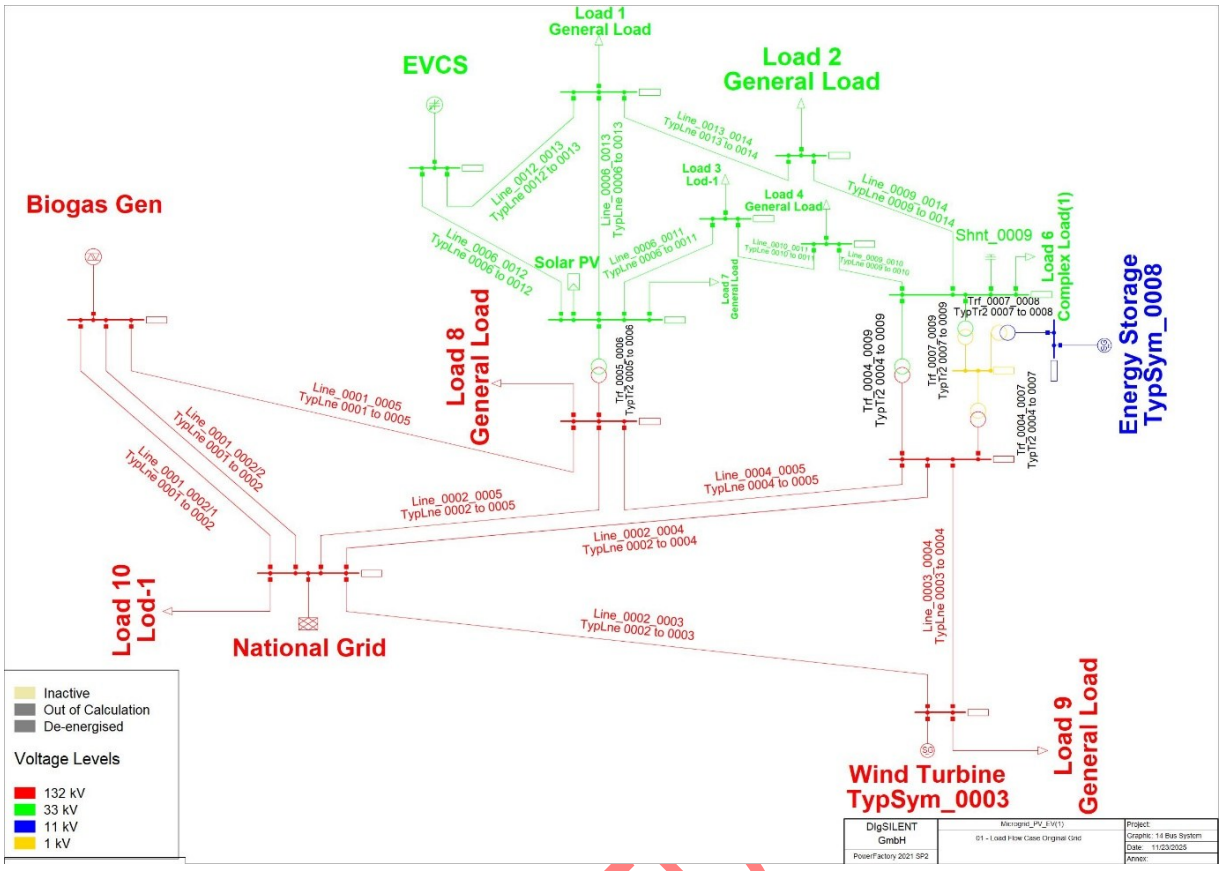

Figure 2. DIgSILENT PowerFactory network model of the hybrid renewable energy system, showing grid interconnection, renewable generation units, energy storage, and aggregated load buses used for reliability analysis.

Power Flow Modelling and Network Equations. Steady-state power flow analysis is formulated using standard AC power flow equations. The net active and reactive power injections at each bus are expressed as given in **Equations (4) and (5):**

$$P_i = \sum_{j=1}^{N} |V_i||V_j|\left(G_{ij}\cos(\theta_i - \theta_j) + B_{ij}\sin(\theta_i - \theta_j)\right) \quad (4)$$

$$Q_i = \sum_{j=1}^{N} |V_i||V_j|\left(G_{ij}\sin(\theta_i - \theta_j) - B_{ij}\cos(\theta_i - \theta_j)\right) \quad (5)$$

where P_i and Q_i are the net active and reactive power injections at bus i, V_i and V_j are the voltage magnitudes, θ_i and θ_j are the voltage phase angles, and G_{ij} and B_{ij} are the elements of the network conductance and susceptance matrices.
These equations are solved numerically in DIgSILENT PowerFactory using standard load-flow algorithms to determine bus voltages and power flows under steady-state conditions, providing the operating point for subsequent dynamic and fault analyses [13], [14].

RESULTS & DISCUSSION

This section presents the results obtained from applying the proposed integrated techno-economic and power system reliability assessment framework for hybrid renewable energy systems (HRES). The analysis evaluates the ability of the methodology to identify cost-optimal system configurations while ensuring stable and reliable operation under varying renewable resource and demand conditions. The results are interpreted not only in terms of system

performance indicators such as cost, renewable penetration, and emissions, but also in terms of their implications for validating the proposed methodological approach. Comparative insights are derived to demonstrate how the framework responds to different resource environments, thereby contributing to a generalized understanding of hybrid system design for remote and ecologically sensitive regions.

Application Scenarios

This section presents the application of the proposed hybrid renewable energy system (HRES) optimization and validation framework to three representative mangrove ecotourism regions. The objective is to evaluate whether the proposed methodology can reliably identify cost-optimal system configurations while ensuring power system stability under diverse resource conditions.

Study Area Selection and Data Inputs. Three mangrove-based ecotourism regions were selected to represent different combinations of resource potential, tourism intensity and energy access constraints in tropical coastal environments: the Sundarbans in Bangladesh, the Can Gio Mangrove Biosphere Reserve in Vietnam, and the Guaratiba mangrove area in Brazil. All three sites feature high ecological value and growing tourism activity, yet face challenges in providing affordable, reliable and low-carbon electricity. The global distribution of mangrove forests and the specific locations of these three case-study sites are illustrated in **Figure** 3**,** highlighting their ecological importance and geographical spread.

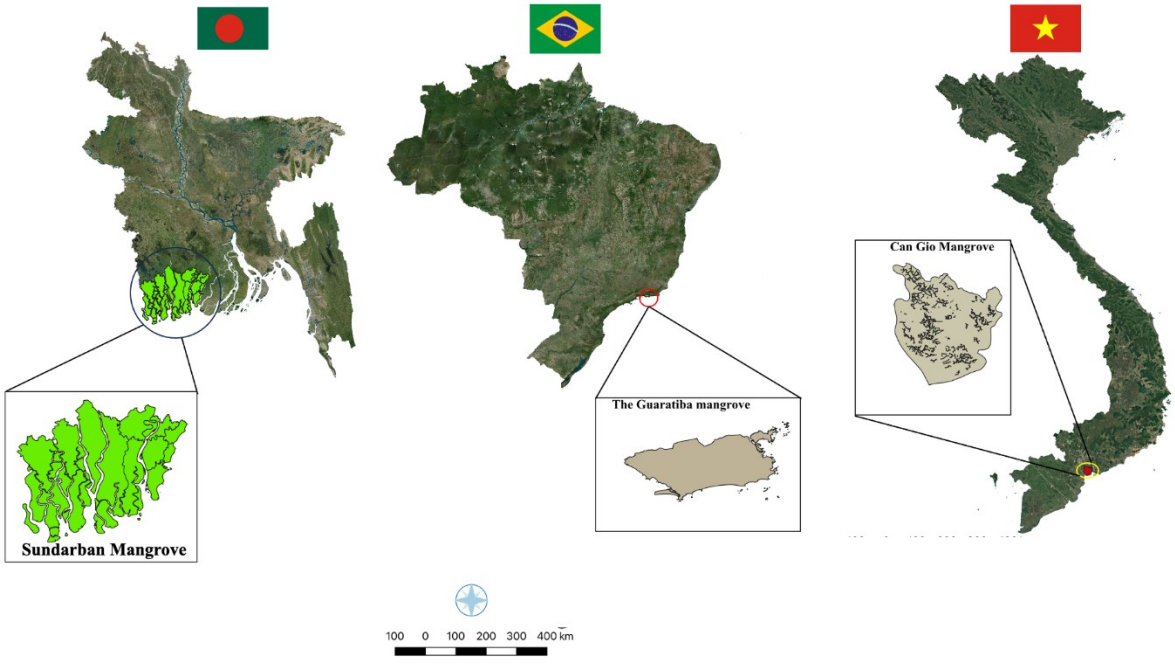

Figure 3. Global Mangrove Distribution and Area of Bangladesh, Vietnam, and Brazil. (Generated by the authors using QGIS based on global mangrove datasets).

Their main characteristics, including renewable resource availability, current energy supply and tourism flows, are summarised in **Table 2.** The following sections provide a detailed overview of each site. All characteristics described in this section represent site-specific inputs adopted for the selected case study locations.

Table 2. Key characteristics of study areas, including geographical, climatic, and energy access parameters for Sundarbans, Can Gio, and Guaratiba.

Parameter	Sundarbans (Bangladesh)	Can Gio (Vietnam)	Guaratiba (Brazil)
Area (km²)	6,000	757.4	36
Avg. GHI (kWh/m²/day)	4.77	5.09	5.14
Avg. Wind Speed (m/s)	8.3	5.23	3.98
Biomass Availability (ton/day)	5.68	4.12	5.13
Grid Access	Poor	Unstable	Limited

Sundarbans, Bangladesh. The first case study is located in the Sundarbans, the world's largest continuous mangrove forest and a UNESCO World Heritage Site, receives approximately 200,000 visitors per year for boat safaris, wildlife observation and visits to small forest and fishing communities, yet remains largely isolated from the national grid and heavily dependent on local diesel generation. Electricity is predominantly supplied by small diesel generator sets and informal mini-grids, with delivered costs exceeding 0.30 USD/kWh due to fuel transport by boat and high maintenance requirements. At the same time, the region exhibits renewable energy resources, with mean wind speeds of about 8.3 m/s (rising to 9–10 m/s during the monsoon), average GHI of roughly 4.95 kWh/m²/day and biomass availability from mangrove pruning and sawmill waste suitable for dispatchable conversion. Harsh environmental conditions, including high humidity, saline air, and tidal variations exceeding 2 m, increase operation and maintenance costs by an estimated 20–25% annually, which must be considered when defining system input parameters for this site.

Can Gio, Vietnam. The second case study focuses on the Can Gio Mangrove Biosphere Reserve, located near the major urban centre of Ho Chi Minh City. It attracts roughly 150,000 tourists per year for mangrove boat tours, homestays, seafood tourism and environmental education, alongside intensive aquaculture and small-scale agriculture. Electricity access is characterised by partial but unstable grid connectivity. Existing grid lines provide basic supply; however, increasing tourism and aquaculture demand has placed pressure on the infrastructure, leading to frequent voltage fluctuations and supply interruptions, which result in the widespread use of diesel generators as backup sources. The region is characterised by average solar irradiance of around 5.14 kWh/m²/day, moderate coastal wind speeds of approximately 5.2 m/s, and biomass resources derived from aquaculture and agricultural residues. These characteristics define the local input conditions for system modelling and analysis.

Guaratiba, Brazil. The third case study is Guaratiba, a conserved mangrove area near Rio de Janeiro, characterized by relatively low wind speeds and higher solar and biomass availability. With approximately 100,000 visitors per year, the region faces typical constraints associated with limited grid access in peripheral coastal zones. The average wind speed is about 4.0 m/s, which limits wind energy utilization, while average solar irradiance is around 4.77 kWh/m²/day. Biomass residues from nearby agricultural and forestry activities constitute an additional local energy resource. These site-specific characteristics are used to define the input parameters for hybrid system configuration in wind-limited coastal environments.

Renewable Resource Characterization. The viability of hybrid renewable energy systems (HRES) depends strongly on the availability and variability of local renewable resources. For the Sundarbans (Bangladesh), Can Gio (Vietnam), and Guaratiba (Brazil), three primary renewable sources were considered: solar, wind, and biomass. Resource data were collected from NASA-SSE, NREL, and national meteorological agencies, then validated against on-site or regional measurements converted into hourly time series for HOMER Pro. A concise cross-site snapshot

of mean values, seasonality cues, and practical implications is summarized in **Table 3** while spatial/temporal distributions are visualized in
Figure 5 **and**
Figure 6 (solar),
Figure 7 (wind), and
Figure 8 (Biomass).

Table 3. Renewable resource assessment summary, presenting solar, wind, and biomass potential with capacity factors across case study locations.

Site	Solar GHI (kWh/m²/day)	Indicative PV CF (%)	Wind speed @50 m (m/s)	Indicative Wind CF (%)	Biomass residues (t/yr)	Biomass potential (kWh/day)
Sundarbans	4.95	18-20	8.3 **(9-10 monsoon)**	28-35	1500	4200
Can Gio	5.14	19-21	5.2	18-22	1200	3600
Guaratiba	4.77	17-19	4.0	12-16	900	2800

Solar energy. Solar resource characterization is based on long-term GHI data for each site. The average daily GHI values adopted for the Sundarbans, Can Gio, and Guaratiba are 4.95 kWh/m²/day, 5.14 kWh/m²/day, and 4.77 kWh/m²/day, respectively, as summarised in **Table 3.** These values are obtained from the Global Solar Atlas for Bangladesh, Vietnam, and Brazil and are cross-checked against national meteorological statistics for consistency.

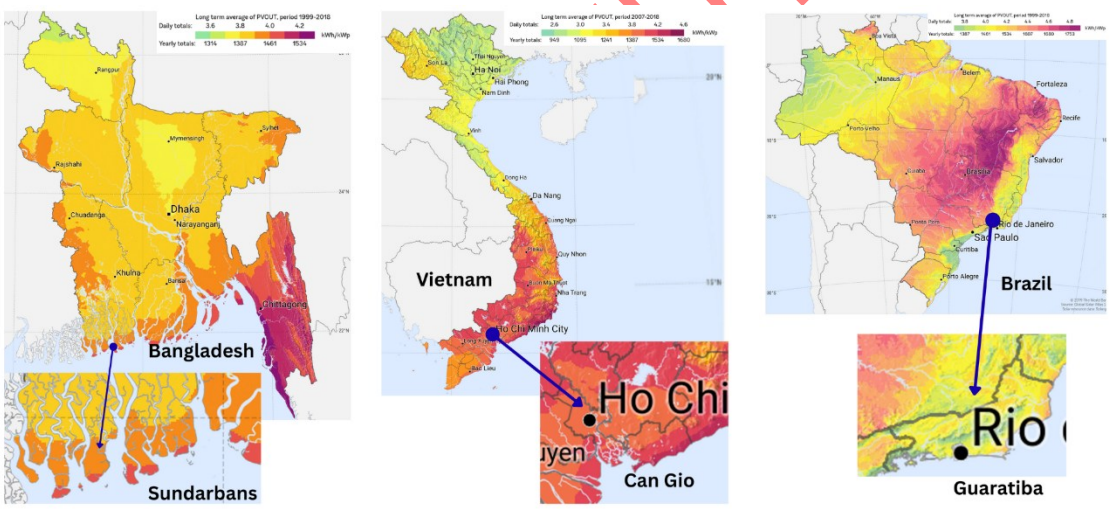

Figure 4. Photovoltaic Power Potential in Sundarbans, Can Gio, and Guaratiba.

Figure 4 illustrates the photovoltaic potential across Sundarbans, Can Gio, and Guaratiba, with average GHI values ranging from 4.77 to 5.14 kWh/m²/day. This indicates that solar energy can serve as the backbone resource for all three sites, while wind and biomass must be integrated to account for variability and provide dispatchable capacity.
To generate the hourly solar input series required for system simulations, the long-term average daily GHI values are combined with representative diurnal profiles for each latitude and with monthly variation patterns derived from the same datasets. This procedure produces hourly time series that preserve typical daily and seasonal variability while remaining consistent with the average values reported in Error! Reference source not found.**.** The monthly average profiles for the three sites are shown in **Figure 5,** and the corresponding clearness indices are presented in **Figure 6.**

Wind Energy. Wind resource characterization is based on mean wind speeds representative of the turbine hub height at each site. The average hub-height wind speeds adopted in this study are 8.3 m/s for Sundarbans (increasing to approximately 9–10 m/s during the monsoon period), 5.2 m/s for Can Gio and 4.0 m/s for Guaratiba, as summarized in Error! Reference source not found.**.** These values are derived from the Global Wind Atlas for coastal locations closest locations near the case study sites and are consistent with regional meteorological observations.

For the selected case study sites, wind speed data available at reference heights (typically 10–30 m) are extrapolated to the assumed hub height using a standard power-law profile with roughness parameters representative of coastal and mangrove terrain. Hourly wind speed series are generated to reflect the adopted mean values and seasonal variation, and are converted into electrical power time series using manufacturer-provided or generic power curves for 70–100 kW horizontal-axis wind turbines suitable for small hybrid systems. Monthly variability in wind resources across the three sites is illustrated in **Figure 7** while Error! Reference source not found. consolidates the key wind statistics adopted for system modelling.

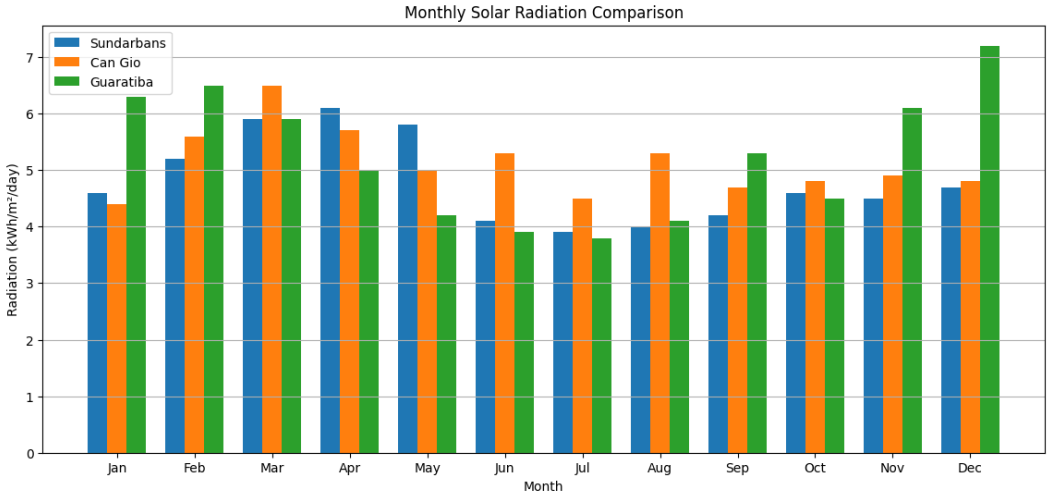

Figure 5. Sundarbans, Can Gio, Guaratiba Monthly Average Solar Global Horizontal Irradiance (GHI).

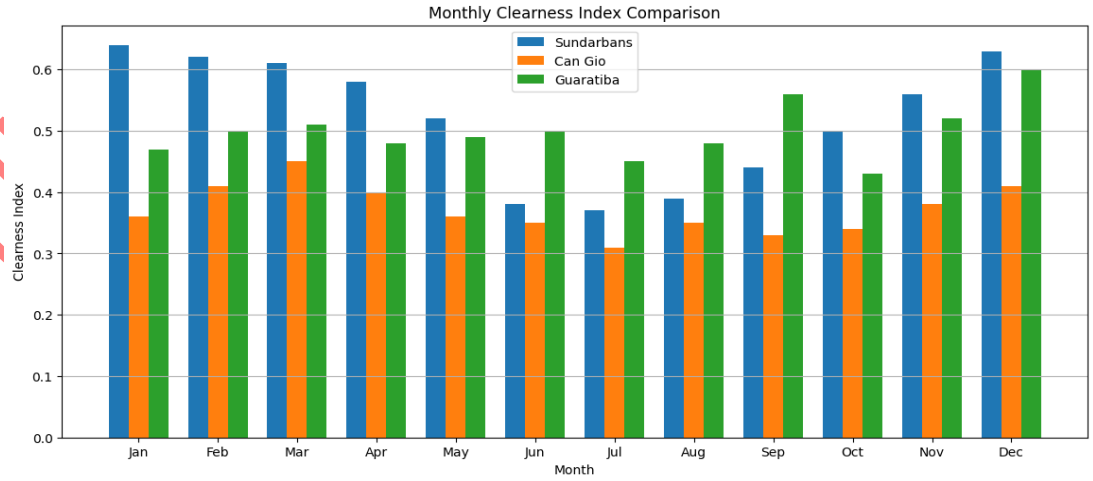

Figure 6. Sundarbans, Can Gio, Guaratiba Monthly Average Clearness Index.

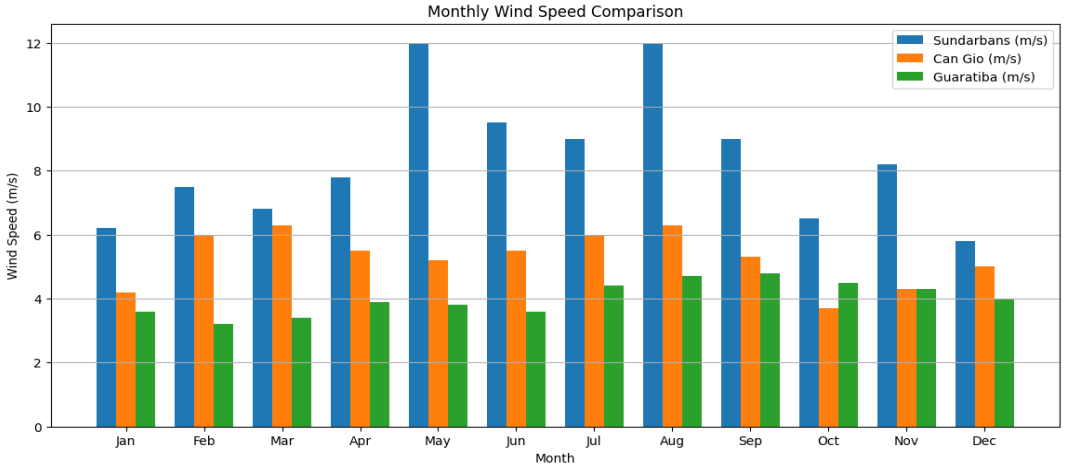

Figure 7. Sundarbans, Can Gio, Guaratiba Monthly Average Wind Speed Data.

Biomass. Biomass resources are characterized by mapping locally available residues and by-products that can be used for energy without undermining environmental or tourism objectives. The three case studies differ in the dominant biomass sources. In Sundarbans, the main resources are mangrove pruning residues and sawmill offcuts from controlled forestry and wood processing. In Can Gio, biomass is primarily associated with aquaculture sludge and fish-processing residues from pond-based production systems. In Guaratiba, agricultural and forestry residues from the surrounding hinterland constitute the principal biomass feedstock.

For each site, annual residue quantities are estimated from activity data, including harvested area, processed volume or aquaculture pond size, combined with residue-to-product ratios reported in biomass and aquaculture studies. On this basis, the annual biomass residue availability is assumed to be 1500 t/yr in Sundarbans, 1200 t/yr in Can Gio and 900 t/yr in Guaratiba, as summarized in Error! Reference source not found.**.** Using typical lower heating values and conversion efficiencies for the selected technologies, these quantities are converted into daily biomass energy potentials of approximately 4200 kWh/day for Sundarbans, 3600 kWh/day for Can Gio and 2800 kWh/day for Guaratiba. These values define the maximum biomass energy availability adopted for system modelling. The comparison of biomass residues and corresponding energy potentials across the three sites is summarised in Error! Reference source not found. and illustrated in **Figure** 8**.**

The adopted biomass availability ranges are consistent with values reported for small coastal and fisheries-oriented communities, where forestry, aquaculture, and agricultural activities generate comparable residue flows. The selection of biomass conversion technologies reflects the dominant residue types and local operating conditions. In the Sundarbans, woody residues are assumed to be processed using a small fixed-bed gasifier coupled to a synchronous generator, a configuration reported in remote community applications. In Can Gio and Guaratiba, organic sludge and mixed agricultural residues are assumed to be treated using anaerobic digesters, with the resulting biogas supplied to gas-engine generators available at comparable scales. The resulting daily biomass energy potentials are used as site-specific input constraints for the techno-economic optimisation.

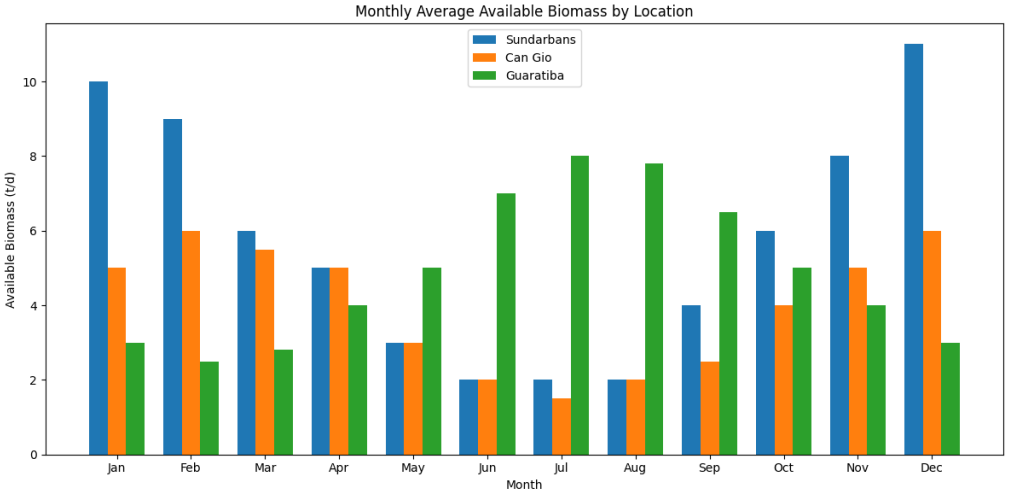

Figure 8. Sundarbans, Can Gio, Guaratiba Monthly Average Available Biomass Data.

Sectoral load modelling. The total electricity demand is divided into residential, agricultural, industrial and service, and electric mobility sectors to capture the diverse consumption patterns of the case study regions. This classification enables a more realistic representation of load profiles and improves the accuracy of techno-economic optimization.

Residential load. Household electricity use in isolated or weak-grid communities with basic services typically lies between 1.5 and 2.5 kWh per day, depending on appliance ownership and comfort level. Studies in tourism-oriented coastal settlements with limited infrastructure report similar magnitudes when lighting, phone charging, fans and a few small appliances are considered. In this study, a daily consumption of 2 kWh per electrified household is adopted, which falls within these reported ranges and reflects a moderate level of service appropriate for the three case study regions. The number of households in each site is shown in **Table 4,** and the resulting residential energy use constitutes a major component of the total demand profile.

Agricultural load. Irrigation and aquaculture pumping are important electricity uses in coastal zones where agriculture and fisheries support local livelihoods and tourism. Energy assessments for small-scale irrigation and aquaculture systems indicate typical daily electricity requirements of about 5–10 kWh per pump, based on motor ratings and operating hours. A value of 7.5 kWh per day per pump is therefore assumed as a representative mid-range figure. The number of agricultural and aquaculture pumps in each case study site is listed in **Table 4**. Their operation is allocated predominantly to late morning and afternoon hours, consistent with irrigation and pond-management practices in similar coastal environments.

Industrial and services load. Small fish-processing units, ice plants and cold-storage facilities are common in coastal tourism and fisheries clusters and contribute to local electricity consumption. Studies of seafood processing industries report daily electricity demands on the order of 150–250 kWh for small facilities, depending on throughput and refrigeration requirements. To represent these activities in the case study regions, a daily demand of 200 kWh per small industrial or service unit is adopted. The number of such units for each site is provided in

Table 4, and their operation is scheduled primarily during daytime and early evening hours, in line with reported processing and storage practices.

Electric mobility load. In emerging ecotourism destinations, electric boats, shuttles or small vehicles are increasingly used for short-distance transport and tours. Real-world tests of battery electric vehicles indicate specific energy consumption values in the range of 15–30 kWh per 100

km, depending on vehicle type, speed and driving conditions. For typical daily travel distances of 40–70 km, this corresponds to approximately 8–12 kWh per day per vehicle. Accordingly, a daily electricity use of 10 kWh per electric vehicle is assumed in this work.
The number of vehicles in each site is given in

Table 4 and their charging is scheduled primarily during late evening and night hours, when vehicles and boats return from tourism and transport activities.

Table 4 summarizes the daily energy consumption and peak load values for each demand sector considered in the three case study regions. The total daily electricity demand across all sectors amounts to 2,935 kWh/day, with a maximum peak load of 578 kW.

Table 4. Sectoral energy demand breakdown for mangrove ecotourism areas, showing daily consumption and peak load contributions.

Sector	Units/ Assumptions	Daily Energy (kWh)	Peak Load
Residential	480 homes × 2 kWh + 20 lodges × 20 kWh	1,360	248
Agricultural	50 pumps × 7.5 kWh	375	80
Industrial	5 units × 200 kWh	1000	200
EV Charging	20 EVs × 10 kWh	200	50
Total		2935 kWh	578 kW

Each sectoral profile is normalized and mapped onto 24 hourly time steps according to these usage patterns. The normalized shapes are then scaled by the sectoral daily energy demands and by the number of units in each category. Finally, the sectoral profiles are summed to produce the composite hourly load curve for each case study region. The resulting profiles exhibit pronounced evening peaks driven by residential and tourism demand, daytime contributions from agricultural and industrial activities, and smaller late-evening increases due to charging of electric mobility, as illustrated in
Figure 9**.**

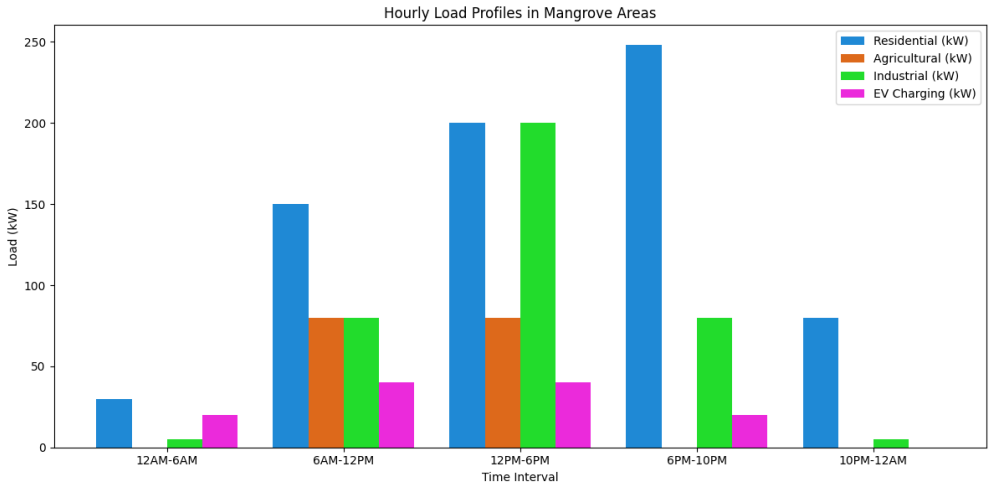

Figure 9. Hourly Load Profile for Residential, Agricultural, Industrial, and EV Charging in Mangrove Tourist Areas.

TECHNO-ECONOMIC PERFORMANCE

This section presents the techno-economic performance of the optimized hybrid renewable energy systems for the selected case study sites. The results include optimal system configurations, component sizing, and key economic indicators such as NPC, LCOE, and

renewable energy penetration. These findings provide insight into the cost-effectiveness and feasibility of hybrid systems under different resource conditions.

Optimal System Configuration and Component Sizing

The optimization results highlight clear contrasts among Sundarbans, Can Gio, and Guaratiba in terms of sizing, cost, and renewable penetration. As shown in **Table 5,** all three sites adopted solar PV capacities between 100–200 kW, supported by modest wind installations (70–100 kW) and small-scale biomass generators (50–100 kW). Battery banks were relatively uniform, ranging from 660 to 713 kWh, ensuring autonomy of one day under average load conditions. These similarities indicate that hybridization follows a common design logic, but the balance between PV, wind, and biomass shifted according to local resources.

Sundarbans, with strong average wind speeds of 8.3 m/s, integrated the highest wind share (100 kW across all load types), reducing the reliance on PV and biomass compared to the other sites. In contrast, Can Gio with only 5.2 m/s average wind relied more heavily on PV (up to 200 kW) and biomass backup. Guaratiba, where wind resources were weakest (4.0 m/s), leaned strongly on PV and biomass, with wind playing only a supplementary role.

Table 5. Optimal component sizing results from HOMER Pro optimization, showing technology capacities by site and load type

Metric	Load Type	Sundarbans	Can Gio	Guaratiba
PV capacity (kW)	Residential	200	200	200
	Industrial	100	200	200
	Agricultural	100	100	100
Wind capacity (kW)	Residential	100	80	70
	Industrial	100	80	70
	Agricultural	100	80	70
Biomass capacity (kW)	Residential	100	50	100
	Industrial	100	50	100
	Agricultural	50	50	50
Battery storage (kWh)	Residential	660	686	713
	Industrial	660	686	713
	Agricultural	660	686	713

Economic Performance Indicators. The techno-economic outcomes are summarized in **Table** 6. The lowest LCOE was achieved in Sundarbans' industrial configuration at 0.112 USD/kWh, demonstrating that strong wind resources directly translate into lower energy costs. Comparable results were reported in coastal communities of Newfoundland, Canada, where hybrid renewable microgrids optimized with HOMER achieved competitive LCOE values while maintaining zero emissions. By comparison, Can Gio showed the highest LCOE, particularly for residential loads (0.215 USD/kWh), reflecting its weaker wind and higher reliance on biomass. Guaratiba's LCOE values were moderate, with residential and industrial loads both at 0.133 USD/kWh, balancing PV and biomass contributions effectively.

NPC followed a similar trend. Sundarbans industrial loads recorded the lowest NPC (1.50M USD), while Sundarbans residential systems required up to 1.82M USD, reflecting larger PV and biomass investments. Can Gio showed slightly higher NPC values (1.47–1.74M USD) due to less favorable wind conditions, while Guaratiba's NPC was lowest overall for agriculture (1.44M USD) owing to modest load requirements.

All optimized systems achieved high renewable penetration (80–85%), with GHG reductions exceeding 70% compared to diesel-only baselines. This confirms that, regardless of site-specific resource differences, hybrid systems provide both economic and environmental gains.

These findings demonstrate that hybridization provides a reliable cost–emission trade-off, but techno-economic feasibility alone is not sufficient. To fully evaluate system robustness, the

optimized configurations were validated in DIgSILENT PowerFactory under dynamic operating conditions.

From an operational perspective, the optimised configurations are able to supply demand even during periods with low solar irradiance and reduced wind output. In such hours, the dispatchable biomass unit operates closer to its rated power, while the battery bank provides short-term peak support, and the diesel generator is used only as a last resort to avoid capacity shortages above the 1% annual limit imposed in HOMER Pro. For example, in the Sundarbans the 100-kW biomass generator combined with 660–713 kWh of storage can cover evening peaks of around 250–300 kW over several hours, with only limited diesel contribution in extreme situations. This behaviour is consistent with the high renewable penetration (80–85%) and the low unmet-load levels implied by the techno-economic optimisation results, as reflected in the key performance indicators presented in

Table 6**,** including NPC, LCOE, and emission reduction.

Table 6. Techno-economic performance indicators of optimized hybrid systems, including NPC, LCOE, and emission reduction

Metric	Load	Sundarbans	Can Gio	Guaratiba
NPC (USD)	Residential	1,815,144	1,738,382	1,616,726
	Industrial	1,496,989	1,574,979	1,616,726
	Agricultural	1,551,142	1,474,478	1,474,478
LCOE (USD/ kWh)	Residential	0.161	0.215	0.133
	Industrial	0.112	0.151	0.133
	Agricultural	0.196	0.189	0.176
Renewable penetration (%)	All loads	85	80	82
GHG reduction (%)	All loads	70	70	70

Sensitivity analysis. To assess the robustness of the optimal designs, a sensitivity analysis is performed on key economic parameters. Diesel fuel price, battery replacement cost and real discount rate are varied within plausible ranges based on recent market data and national energy statistics for the three countries. For each parameter combination, the optimization is repeated and the resulting technology mixes and LCOE values are recorded. This analysis shows how changes in fuel prices, capital costs and financing conditions affect system cost and technology choice, and whether the hybrid options remain more attractive than the diesel-only reference. The detailed sensitivity trends are discussed qualitatively here, while quantitative impacts are reflected in the variation of LCOE values reported in

Table 6.

Power System Reliability and Dynamic Performance

The optimized systems were validated in DIgSILENT PowerFactory to ensure that their techno-economic feasibility **(Table 5 and**

Table 6**)** is supported by technical robustness. The model layout is shown in

Figure 2, while detailed reliability indicators are summarized in **Table 7.** Representative transient responses are provided in **Figure 11, Figure** 12**, Figure** 13**, and Figure** 14**,** focusing on the Sundarbans (wind-rich) and Guaratiba (PV–biomass dominant).

Steady-State Load Flow Results. From these simulations, several reliability and power-quality metrics are extracted, including maximum voltage deviation during and after the disturbance, peak line loading, maximum active and reactive power losses and fault recovery time. Fault recovery time is defined as the duration required for system frequency and bus voltages to return to acceptable bands around their nominal values after fault clearing. These indicators are compared across the three case study sites to evaluate how resource mixes and system

architectures influence dynamic stability in addition to techno-economic performance, and the main results are summarized in **Table 7.**

Table 7. Power system reliability metrics from DIgSILENT validation, demonstrating voltage stability, loss factors, and fault recovery performance.

Metric	Sundarbans	Can Gio	Guaratiba
Voltage Deviation (±%)	<5%	<5%	<5%
Max Line Loading (%)	70%	65%	60%
Active Power Loss (%)	1.9	2.1	2.0
Reactive Power Loss (%)	1.3	1.1	1.0
Fault Recovery Time (s)	1.8	2.0	1.7

Dynamic Fault Response and Stability Analysis. To assess the dynamic response of the optimized hybrid systems under disturbed conditions, three-phase short-circuit faults are simulated in DIgSILENT PowerFactory. For each case study site, a fault is applied at the main busbar of the distribution network model and cleared after a short duration representative of realistic protection clearing times. Time-domain simulations are then performed to obtain the evolution of generator active power, system frequency and bus voltages during the fault and subsequent recovery period.

Figure 10 shows the active power response during and after the three-phase fault for the three sites, indicating a rapid and well-damped recovery. The corresponding frequency response in **Figure** 11 remains within acceptable limits and returns close to nominal within about 2 s, consistent with the recovery times reported in **Table 7.** The bus voltage profiles in **Figure** 12 stay within approximately ±5% of nominal during the fault and restoration period, while **Figure** 13 illustrates reactive power support from the generators and converters, confirming that line and voltage limits are respected under disturbed conditions.

In the Sundarbans, where renewable penetration exceeded 85%, the active power response **(Figure** 10**)** showed a sharp but well-damped recovery supported by strong wind and battery interaction. The system frequency **(Figure** 11**)** stabilized within 1.7–1.8 seconds, while bus voltage **(Figure** 12**)** remained within ±5% of nominal throughout the distribution period. Losses were modest, with active losses 1.9% and reactive losses 1.2%, confirming that high renewable integration did not compromise stability.

In Guaratiba, with renewable penetration around 82%, the active power curve **(Figure** 10**)** recovered slightly more slowly due to limited wind potential but still stabilized effectively. Frequency **(Figure** 11**)** returned to nominal in 1.8 seconds, and voltage **(Figure** 12**)** remained within the ±5% threshold. Losses were comparable to Sundarbans, with active losses 2.0% and reactive losses 1.3%.

Can Gio, representing an intermediate case with 80% renewable penetration, showed slightly longer recovery (2.0 seconds) due to moderate wind contribution, and voltage deviations were slightly higher than Sundarbans but still within ±5%. Losses were similar to the other two sites, with active and reactive values consistent with **Table 7.**

Across all three sites, line loading remained below 70%, active power losses did not exceed 2.1%, reactive losses stayed under 1.3%, and fault recovery times were under 2.0 seconds.

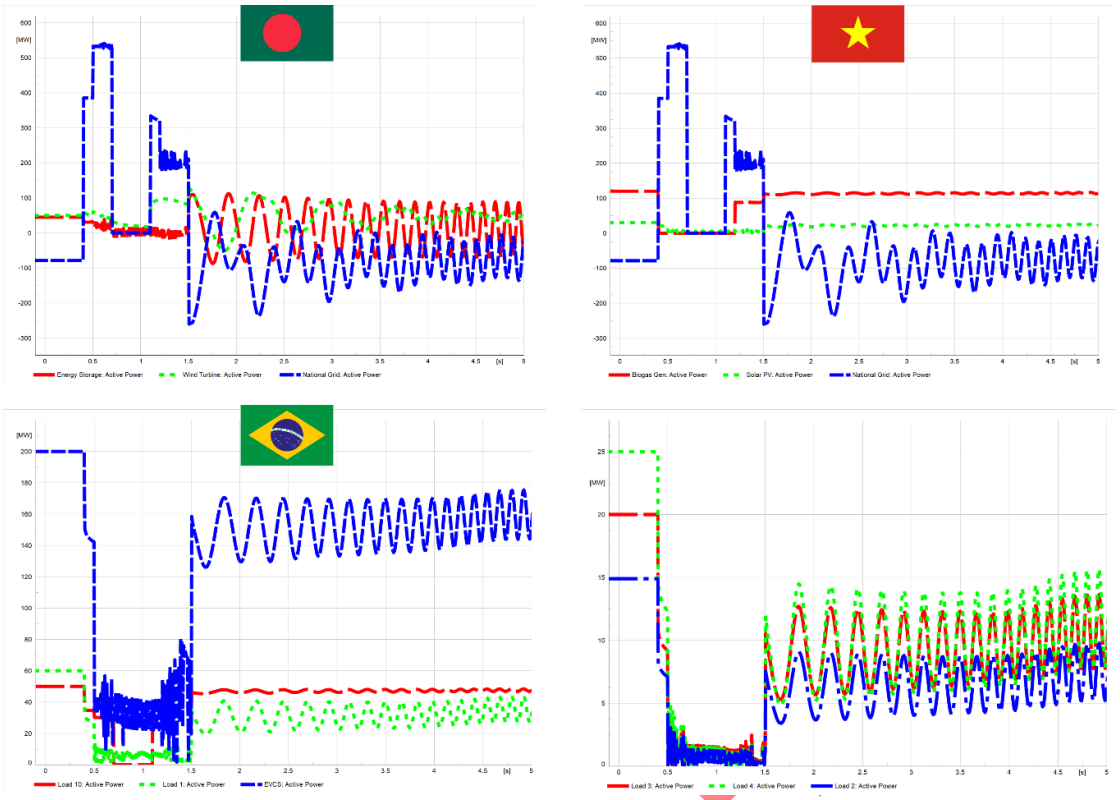

Figure 10. Active power response of the system during a three-phase fault and recovery in three study areas.

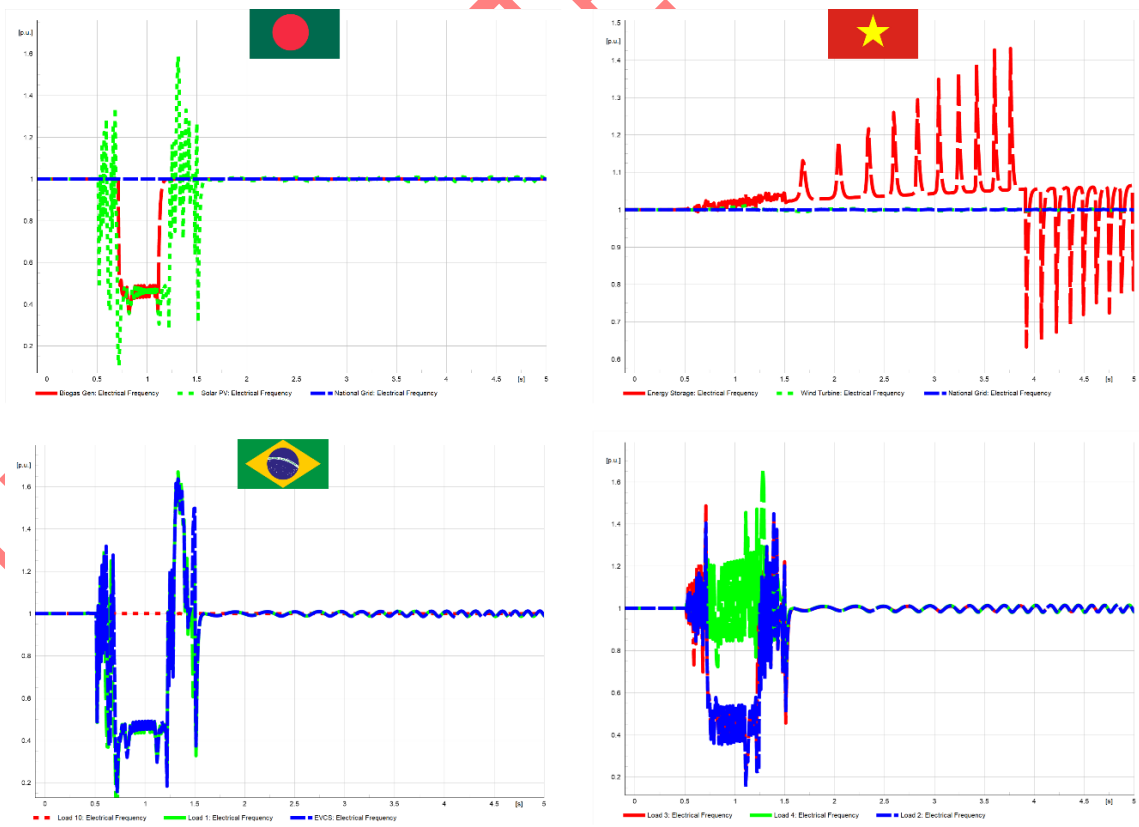

Figure 11. Frequency response of the Sundarbans system during a three-phase fault and recovery, showing restoration within 2 seconds.

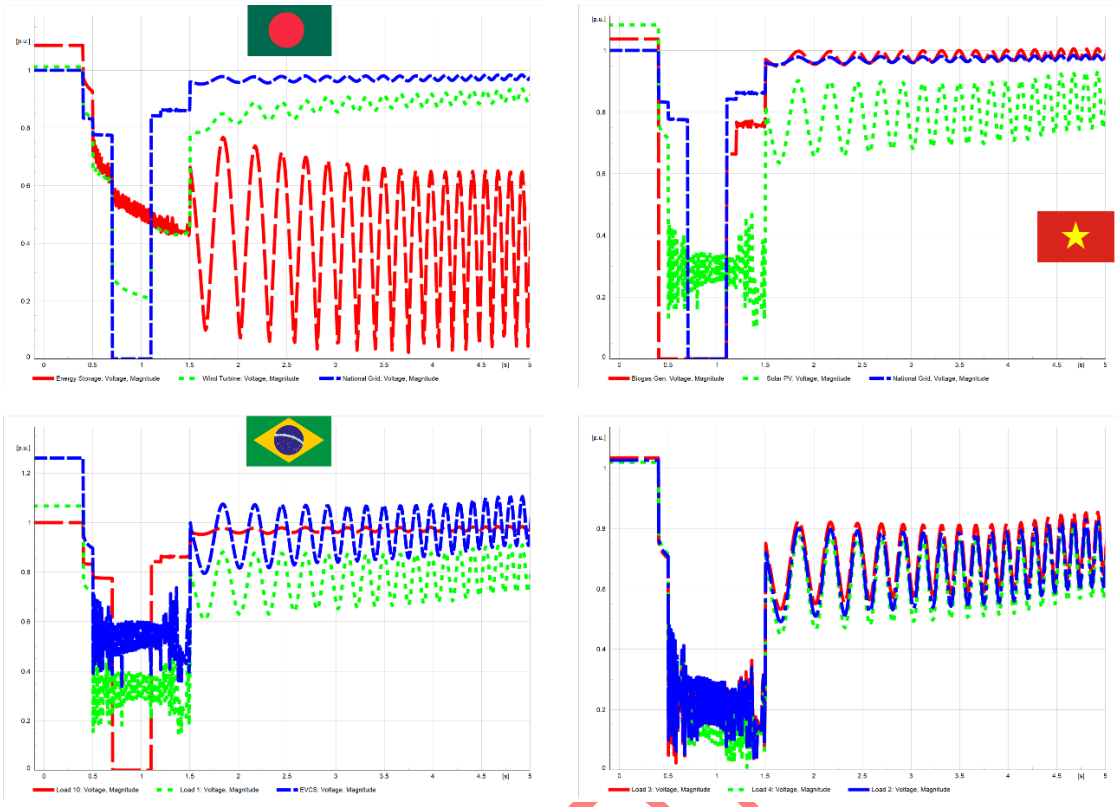

Figure 12. Bus voltage profile of the Sundarbans system during a three-phase fault and recovery, remaining within ±5% of nominal voltage.

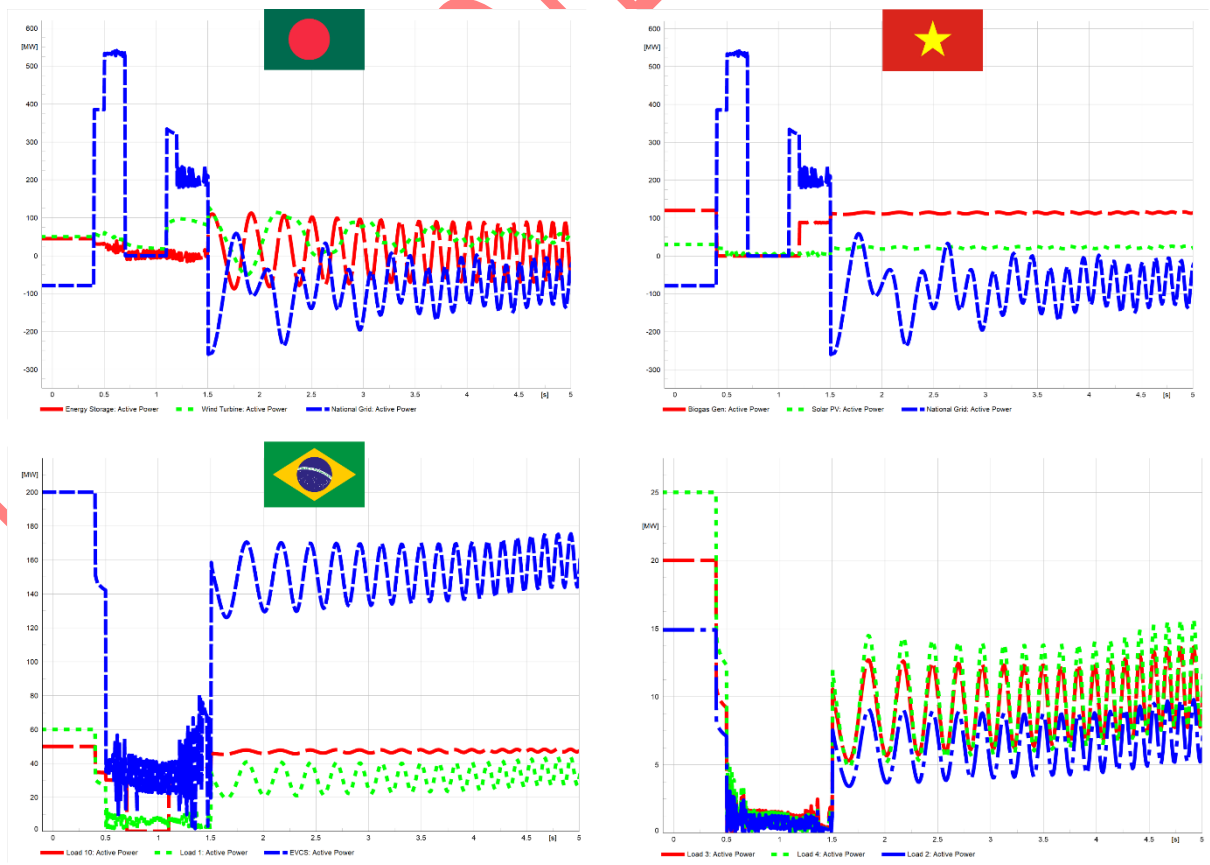

Figure 13. Reactive power profile of the system across the three case study sites.

Comparative Insight and Policy Implications

A comparative view of the three case studies highlights how resource availability shapes both techno-economic performance and system reliability. Sundarbans, with its strong wind regime (8.3 m/s), consistently achieved the lowest LCOE (0.112 USD/kWh for industrial loads) and high renewable penetration (85%). Guaratiba, where wind is limited (4.0 m/s), relied more on PV and biomass but still delivered competitive costs (0.133 USD/kWh for residential and industrial loads) with strong reliability indicators. Can Gio, by contrast, faced the highest LCOE (0.215 USD/kWh for residential loads) due to its moderate wind (5.2 m/s) and dependence on biomass.

Despite these differences, the reliability assessment confirmed that all three sites maintain voltage deviations within ±5%, losses below 2.1%, and fault recovery within two seconds. These consistent outcomes suggest that hybrid renewable systems can be scaled across diverse mangrove regions without compromising stability, provided proper component sizing and storage integration are ensured.

From a policy perspective, these findings carry three important implications. First, resource-tailored system design is essential: wind-rich Sundarbans should prioritize wind integration, while Can Gio and Guaratiba require stronger PV–biomass hybrids. Second, diesel displacement is feasible and impactful: in all sites, renewable penetration exceeded 80% and GHG reductions surpassed 70%, directly supporting national climate commitments. Third, investment frameworks must account for site-specific costs: while LCOE varies between 0.112 and 0.215 USD/kWh, all values remain competitive against isolated diesel systems (often >0.30 USD/kWh), making hybridization an economically rational choice for ecotourism electrification.

These LCOE values are not directly comparable with those of utility-scale PV or wind plants, which benefit from larger scale and standardised technologies. Instead, they should be interpreted relative to existing diesel-based supply in small, isolated tourism sites, where generation costs often exceed 0.30 USD/kWh due to fuel transport and maintenance in harsh coastal environments. Within this context, the LCOE range of 0.112–0.215 USD/kWh indicates that the proposed hybrid systems are economically attractive for remote mangrove ecotourism regions.

Overall, the comparative analysis confirms that hybrid renewable microgrids can deliver affordable, reliable, and low-carbon power in mangrove ecotourism contexts. Policymakers and planners can build on these insights to promote targeted investment, strengthen regulatory support for hybrid systems, and reduce diesel dependence in environmentally sensitive coastal zones.

Link to Sustainable Development Goals

The optimized hybrid systems have direct implications for several Sustainable Development Goals (SDGs), particularly in the context of remote mangrove ecotourism regions. By reducing the Levelized Cost of Electricity to approximately 0.11–0.21 USD/kWh and lowering total energy costs by around 22–35% relative to diesel-only supply, the proposed configurations advance SDG 7 (Affordable and Clean Energy) through the provision of more reliable and cost-effective electricity for tourism facilities and surrounding communities. The high renewable penetration of roughly 80–85% and the strong reduction in diesel dependence contribute to SDG 13 (Climate Action), as annual greenhouse gas emissions are cut by more than 70% compared with existing diesel-based systems in the three sites. These aggregated contributions to SDG 7 and SDG 13, together with the broader social and environmental co-benefits, are summarised in

Figure 14**.**

These improvements in energy affordability and reliability also support local economic development pathways consistent with SDG 8 (Decent Work and Economic Growth). Stable

and cleaner power supply can enhance the quality of tourism services, reduce the risk of business interruption due to outages and fuel shortages, and create new employment opportunities in system installation, operation and maintenance. At the same time, the deployment of decentralized hybrid systems in harsh coastal environments aligns with SDG 9 (Industry, Innovation and Infrastructure), by promoting resilient, low-carbon energy infrastructure and encouraging innovation in the planning and management of off-grid systems for ecotourism and coastal communities.

Finally, by reducing local air and noise pollution, limiting the risk of fuel spills and enabling low-carbon operation of tourism activities, the hybrid systems help to safeguard the ecological integrity of sensitive mangrove ecosystems, thereby contributing to SDG 15 (Life on Land). In combination, the techno-economic and reliability results suggest that carefully designed hybrid renewable energy systems can play a strategic role in aligning ecotourism development with climate and biodiversity objectives in remote mangrove regions. This integrated perspective on SDG 7, 8, 9, 13 and 15 is explicitly illustrated in
Figure 14**,** which links the main techno-economic and environmental outcomes of the proposed systems to their corresponding development targets.

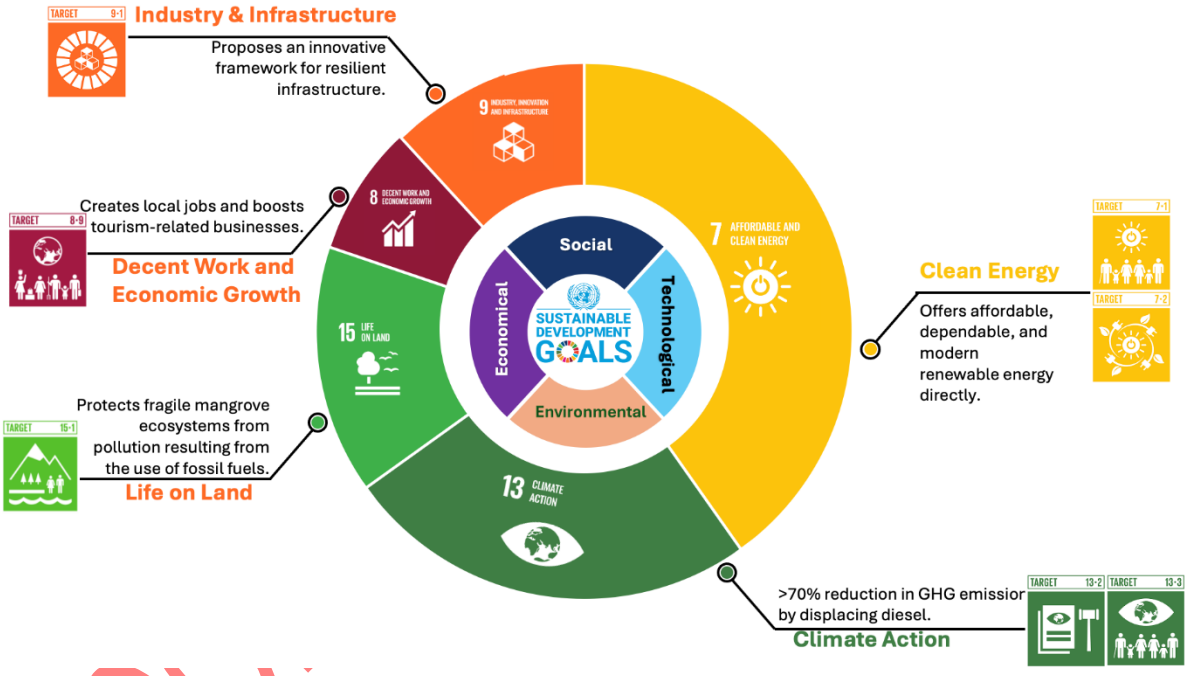

Figure 14. Linkage of hybrid renewable energy systems for mangrove ecotourism with the Sustainable Development Goals (SDG 7, SDG 8, SDG 9, SDG 13, and SDG 15).

CONCLUSION AND FUTURE WORK

This study has shown that carefully designed hybrid renewable energy systems can provide reliable, low-carbon electricity for mangrove-based ecotourism regions with limited or unstable grid access, while also supporting broader sustainable development objectives. Using multi-sector load profiles and site-specific solar, wind and biomass resource assessments for the Sundarbans (Bangladesh), Can Gio (Vietnam) and Guaratiba (Brazil), techno-economic optimisation in HOMER Pro identified photovoltaic–wind–biomass–battery configurations that achieve high renewable penetration of approximately 80–85%, reduce total energy costs by about 22–35% compared with diesel-only supply and deliver LCOE in the range of roughly 0.11–0.21 USD/kWh. These hybrid systems also cut annual greenhouse gas emissions by more than 70% relative to current diesel-based practice, while load-flow and dynamic simulations in DIgSILENT PowerFactory confirm that bus voltages remain within acceptable limits, line

loadings stay comfortably below thermal ratings and three-phase faults are cleared with well-damped recovery of power, frequency and voltage in a few seconds. Together, these results indicate that hybrid renewable systems represent a technically feasible and economically attractive alternative to diesel generation in remote mangrove ecotourism regions, contributing directly to SDG 7 (Affordable and Clean Energy) and SDG 13 (Climate Action), while supporting biodiversity protection in sensitive mangrove ecosystems (SDG 15) and creating conditions for greener local economic development and resilient infrastructure (SDGs 8 and 9). At the same time, the analysis is constrained by the use of survey-based demand estimates, satellite and reanalysis resource data, simplified dispatch and network representations and uncertain long-term cost and financing parameters, so the reported indicators should be viewed as indicative rather than exact and refined with site-specific measurements before implementation. Future work should therefore focus on integrating advanced control and demand-side management strategies, probabilistic and scenario-based reliability assessments, and more detailed protection and black-start modelling, as well as examining innovative business models, tariff structures and financing mechanisms suitable for community-based ecotourism contexts; in parallel, life-cycle assessment of technologies and valuation of ecosystem services would help to clarify the full environmental and socio-economic benefits of hybrid renewable energy systems in mangrove regions.

ACKNOWLEDGEMENT

The authors extend their appreciation to the Deanship of Scientific Research at Northern Border University, Arar, KSA, for funding this research work through the project number "NBU-FFR-2026-3623-06".

APPENDIX

The component costs used in HOMER Pro optimization are summarized in **Appendix 1.** These were derived from regional benchmarks, vendor data, and published techno-economic studies for coastal and mangrove environments. All values are reported in 2025 (USD). This comprehensive nomenclature table in

Appendix 2 will serve as a valuable reference for readers, enabling them to understand the mathematical models in this research paper and making it more accessible and professionally presented.

Appendix 1. Component cost assumptions for HOMER Pro optimization, based on 2023 USD values and regional market conditions.

Component	Capital Cost	Replacement cost	O & M Cost	Notes
Solar PV	600 USD/kW		10 USD/kW·yr	Based on regional benchmarks
Wind turbine (10 kW)	40,000 USD/unit		500–1,000 USD/yr	Costs vary with corrosion risk in coastal zones
Biogas generator	1,000 USD/kW		0.10 USD/kWh	Includes biomass collection & processing
Battery (13.2 kWh, 220V)	6,500 USD/unit	6,000 USD/unit	5 USD/kW·yr	Lithium-ion technology
Bi-directional inverter	266 USD/kW		5 USD/kW·yr	Required for AC/DC integration
Grid electricity	0.10 USD/kWh (purchase)		0.05 USD/kWh (sellback)	Regional tariff assumption

Values adapted from recent techno-economic studies of hybrid renewable energy systems [39], [40] and adjusted using indicative regional price information for Bangladesh, Viet Nam and Brazil [15].

Appendix 2. Notation for mathematical equation used

Symbol	Description	Unit	Symbol	Description	Unit
LCOE	Levelized Cost of Energy	USD/kWh	RF	Renewable penetration (share of energy supplied by PV, wind and biomass)	–
NPC	Net Present Cost	USD	P_i	Active power at bus i	kW
Ct	Total cost in year *t* (investment, replacement, fuel and O&M)	USD/year	Q_i	Reactive power at bus i	kVAr
$O\&M_t$	Operation and maintenance cost in year t	USD	V_i, V_j	Voltage magnitudes at buses i and j	kV
F_t	Fuel cost in year t	USD	θ_{ij}	Voltage angle difference between buses i and j	radians
E_t	Energy generated in year t	kWh	G_{ij}	Conductance of line ij	Siemens
E_{PV}	Annual electrical energy generated by the photovoltaic array	kWh/year	B_{ij}	Susceptance of line ij	Siemens
E_{wind}	Annual electrical energy generated by wind turbines	kWh/year	n	Number of buses in the network	–
$E_{biomass}$	Annual electrical energy generated by the biomass unit	kWh/year	i,j	Indices of sending and receiving buses	–
E_{served}	Total annual electrical energy served to the load	kWh/year	Pgen	Generator active power	kW
r	Real discount rate	– (or %)	f	System frequency	Hz
N	Project lifetime (number of years)	Years	Vbus	Bus voltage magnitude	p.u. or kV
t	Year index in the project lifetime (1…N)	–			

REFERENCES

1. Alongi, D.M., *Present state and future of the world's mangrove forests.* Environmental conservation, 2002. 29(3): p. 331-349, https://doi.org/10.1017/S0376892902000231.
2. Donato, D.C., et al., *Mangroves among the most carbon-rich forests in the tropics.* Nature geoscience, 2011. 4(5): p. 293-297, https://doi.org/10.1038/ngeo1123.
3. Ahmed, I., M.A. Razzak, and F. Ahmed, *Sustainable hybrid renewable energy management system for a community in island: A model approach utilising Hybrid Optimization of Multiple Energy Resources optimization and priority setting-based Supervisory Control and Data Acquisition operation.* IET Smart Grid, 2024. 7(6): p. 940-966, https://doi.org/10.1049/stg2.12192.
4. Uddin, M., H. Mo, and D. Dong, *Cost-Effective Design of Grid-tied Community Microgrid.* arXiv preprint arXiv:2503.07414, 2025, https://doi.org/10.48550/arXiv.2503.07414.
5. Ali, M.F., et al., *Economic and Environmental Benefits of Grid-Connected PV-Biomass Systems in a Bangladeshi University: A HOMER Pro Approach.* International Transactions on Electrical Energy Systems, 2025. 2025(1): p. 5053853, https://doi.org/10.1155/etep/5053853.
6. Shezan, S.A., et al., *Design and implementation of an islanded hybrid microgrid system for a large resort center for Penang Island with the proper application of excess energy.*

Environmental Progress & Sustainable Energy, 2021. 40(4): p. e13584, https://doi.org/10.1002/ep.13584Digital Object Identifier (DOI).
7. Islam, M.A., et al., *Optimizing energy solutions: A techno-economic analysis of solar-wind hybrid power generation in the coastal regions of Bangladesh.* Energy Conversion and Management: X, 2024. 22: p. 100605, https://doi.org/10.1016/j.ecmx.2024.100605.
8. Faisal, A. and N. Anwer, *Optimization and techno-economic analysis of hybrid renewable energy systems for the electrification of remote areas.* Wind Engineering, 2024. 48(3): p. 365-383, https://doi.org/10.1177/0309524X231210266.
9. Ahmed, P., et al., *Feasibility and techno-economic evaluation of hybrid photovoltaic system: A rural healthcare center in bangladesh.* Sustainability, 2023. 15(2): p. 1362, https://doi.org/10.3390/su15021362.
10. Prasetyo, S.D., et al., *Techno-economic evaluation of hybrid photovoltaic-wind energy systems for Indonesian government buildings.* J. Sustain. Energy, 2023. 2(3): p. 132-144, https://doi.org/10.56578/jse020303.
11. AbdElrazek, A.S., M. Soliman, and M. Khalid, Evaluating the Techno-Economic Viability of a Solar PV-Wind Turbine Hybrid System with Battery Storage for an Electric Vehicle Charging Station in Khobar, Saudi Arabia. arXiv preprint arXiv:2502.05654, 2025, https://doi.org/10.48550/arXiv.2502.05654.
12. Samatar, A.M., et al., *Techno-economic and environmental analysis of a fully renewable hybrid energy system for sustainable power infrastructure advancement.* Scientific Reports, 2025. 15(1): p. 12140, https://doi.org/10.1038/s41598-025-96401-z.
13. Pan, S., et al. *Optimal placement and power supply of distributed generation to minimize power losses*. in *2023 IEEE International Conference on Communications, Control, and Computing Technologies for Smart Grids (SmartGridComm)*. 2023. IEEE, 10.1109/SmartGridComm57358.2023.10333910.
14. Van Der Meer, A.A., et al. Towards scalable FMI-based co-simulation of wind energy systems using powerfactory. in 2019 IEEE PES Innovative Smart Grid Technologies Europe (ISGT-Europe). 2019. IEEE, https://doi.org/10.48550/arXiv.2309.15727.
15. Islam, M.S., et al., *Techno-economic optimization of a zero emission energy system for a coastal community in Newfoundland, Canada.* Energy, 2021. 220: p. 119709, https://doi.org/10.1016/j.energy.2020.119709.
16. Jahangir, M.H. and R. Cheraghi, *Economic and environmental assessment of solar-wind-biomass hybrid renewable energy system supplying rural settlement load.* Sustainable Energy Technologies and Assessments, 2020. 42: p. 100895, https://doi.org/10.1016/j.seta.2020.100895.
17. He, W., et al., *Optimal analysis of a hybrid renewable power system for a remote island.* Renewable Energy, 2021. 179: p. 96-104, https://doi.org/10.1016/j.renene.2021.07.034.
18. El Hassani, S., et al., *Techno-economic feasibility and performance analysis of an islanded hybrid renewable energy system with hydrogen storage in Morocco.* Journal of Energy Storage, 2023. 68: p. 107853, https://doi.org/10.1016/j.est.2023.107853.
19. Palanichamy, C., T.W. Wen, and P. Naveen, *A microgrid for the secluded Paana Theertham Kani settlement in India.* Clean Energy, 2022. 6(1): p. 43-58, https://doi.org/10.1093/ce/zkac030.
20. Ayan, O. and B.E. Turkay, *Techno-economic comparative analysis of grid-connected and islanded hybrid renewable energy systems in 7 climate regions, Turkey.* IEEE Access, 2023. 11: p. 48797-48825, 10.1109/ACCESS.2023.3276776.
21. Barakat, S., H. Ibrahim, and A.A. Elbaset, *Multi-objective optimization of grid-connected PV-wind hybrid system considering reliability, cost, and environmental aspects.* Sustainable Cities and Society, 2020. 60: p. 102178, https://doi.org/10.1016/j.scs.2020.102178.
22. Ali, Z., et al., *Applications of energy storage systems in enhancing energy management and access in microgrids: a review. Energies. 2023; 16 (16): 5930, https://doi.org/10.3390/en16165930*.
23. Kumar, P. and S. Deokar, *Designing and simulation tools of renewable energy systems: review literature.* Progress in Advanced Computing and Intelligent Engineering: Proceedings of ICACIE 2016, Volume 1, 2018: p. 315-324, https://doi.org/10.1007/978-981-10-6872-0_29.
24. Rasel Ahmed, M., et al., *Assessment of a grid-connected microgrid for suburban areas and EV loads with battery storage during planned grid outages using DIgSILENT powerfactory.*

Electrical Engineering, 2025. 107(12): p. 15069-15098, https://doi.org/10.1007/s00202-025-03336-9.
25. Jiménez-Ruiz, J., A. Honrubia-Escribano, and E. Gómez-Lázaro, *Combined use of Python and DIgSILENT PowerFactory to analyse power systems with large amounts of variable renewable generation.* Electronics, 2024. 13(11): p. 2134, https://doi.org/10.3390/electronics13112134.
26. Herraiz-Cañete, Á., et al., *Forecasting energy demand in isolated rural communities: A comparison between deterministic and stochastic approaches.* Energy for Sustainable Development, 2022. 66: p. 101-116, https://doi.org/10.1016/j.esd.2021.11.007.
27. Gambino, V., et al., *Methodology for the energy need assessment to effectively design and deploy mini-grids for rural electrification.* Energies, 2019. 12(3): p. 574, https://doi.org/10.3390/en12030574.
28. Badiola, M., et al., *Energy use in recirculating aquaculture systems (RAS): a review.* Aquacultural engineering, 2018. 81: p. 57-70, https://doi.org/10.1016/j.aquaeng.2018.03.003.
29. Hartvigsson, E., et al., *Linking household and productive use of electricity with mini-grid dimensioning and operation.* Energy for Sustainable Development, 2021. 60: p. 82-89, https://doi.org/10.1016/j.esd.2020.12.004.
30. Murali, S., et al., *Energy and water consumption pattern in seafood processing industries and its optimization methodologies.* Cleaner Engineering and Technology, 2021. 4: p. 100242, https://doi.org/10.1016/j.clet.2021.100242.
31. Weiss, M., et al., *Energy consumption of electric vehicles in Europe.* Sustainability, 2024. 16(17): p. 7529, https://doi.org/10.3390/su16177529.
32. Davis, N.N., et al., *The Global Wind Atlas: A high-resolution dataset of climatologies and associated web-based application.* Bulletin of the American Meteorological Society, 2023. 104(8): p. E1507-E1525, https://doi.org/10.1175/BAMS-D-21-0075.1.
33. Atlas, G.S., *Validation Report*. 2019.
34. Atlas, G.S., *Solar resource and PV power potential maps and GIS data*. 2016.
35. Badger, J., et al., *The Global Wind Atlas: An eudp project carried out by dtu wind energy, Technical Report, DTU Wind Energy*, 2015.
36. Bujas, T., et al., *Review of energy consumption by the fish farming and processing industry in Croatia and the potential for zero-emissions aquaculture.* Energies, 2022. 15(21): p. 8197, https://doi.org/10.3390/en15218197.
37. Freeman, M., et al., *Offshore aquaculture: a market for ocean renewable energy.* Report for Ocean Energy Systems (OES), 2022.
38. Troell, M., et al., *Aquaculture and energy use.* Encyclopedia of energy, 2004. 1: p. 97-108, https://doi.org/10.1016/B0-12-176480-X/00205-9.
39. Ross-Hopley, D., L. Ugwu, and H. Ibrahim, *Review of Techno-Economic Analysis Studies Using HOMER Pro Software.* Engineering Proceedings, 2024. 76(1): p. 94, https://doi.org/10.3390/engproc2024076094.
40. Kumar, P.H., et al., *Prefeasibility techno-economic analysis of hybrid renewable energy system.* e-Prime-Advances in Electrical Engineering, Electronics and Energy, 2024. 7: p. 100443, https://doi.org/10.1016/j.prime.2024.100443.
41. Ali, Z.M., et al., *Applications of energy storage systems in enhancing energy management and access in microgrids: A review.* Energies, 2023. 16(16): p. 5930, https://doi.org/10.3390/en16165930.